JTTEE5 11:461-467

High Temperature Oxidation of HFPD Thermal-Sprayed MCrAlY Coatings in Simulated Gas Turbine Environments

F.J. Belzunce, V. Higuera, S. Poveda, and A. Carriles

(Submitted 22 February 2001; in revised form 25 May 2001)

NiCrAlY and CoNiCrAlY powders were thermal-sprayed using the high frequency pulse detonation method (HFPD) onto AISI 310 austenitic stainless steel samples to obtain dense, adherent, high temperature oxidation resistant coatings. The oxidation behavior of both types of coatings in a 1000 °C simulated gas turbine environment was experimentally determined. The porosity, hardness, coating thickness, and microstructure were not significantly modified by the high temperature oxidation cycles, but the internal oxidation increases significantly after a very low oxidation time. Surface phase composition was evaluated using x-ray diffraction (XRD) and scanning electron microscope (SEM) techniques, revealing the formation of a continuous and highly protective alumina layer. The oxidation kinetics of both coatings can be characterized by parabolic rate constants, which are very close to those for the formation of aluminum oxide on nickel or cobalt based alloys at similar conditions.

Keywords detonation process, gas turbine environment oxidation, MCrAlY coatings, thermal-sprayed coatings

1. Introduction

Gas-fired gas turbine combined-cycle systems are expected to account for a significant proportion of the projected new electricity generation units to be constructed over the next 10 years. Such plants are available in a range of sizes of up to more than 200 MW per turbine and current combined-cycle plants have professed cycle efficiencies on the order of 49% and are capable of achieving environmental compliance for SO_2 and NO_x. The ultimate goal of these new systems is to reduce the cost of electricity by at least 10%.[1]

To achieve the aforementioned goals, the gas turbine industry is making the utmost effort to allow increased firing temperatures so as to improve engine efficiency and is also using a reduced cooling air/fuel ratio. At the same time, increasing efficiency reduces fuel consumption and therefore reduces emissions of nitrogen oxides (NO_x), carbon monoxide, and hydrocarbons to meet the expected lower limits for pollution in the future.[2]

The main requirements for land-based gas turbines are long life, maximum efficiency, reliability, and minimum cost. The durability of a gas turbine is limited by components operating at high temperatures.[3] Ni-based superalloys are the materials normally used for first stage blades, which operate at the highest gas temperature. The oxidation and high temperature corrosion of these nickel based alloy components is improved by the application of protective coatings. MCrAlY coatings (M = Ni, Co or both) are used worldwide for this purpose. They owe their protective effect to the fact that they form a continuous thermally stable oxide layer on the coating surface. These coatings are usually applied using vacuum plasma-spray (VPS) or electron beam physical vapor deposition (EB-PVD) processes. Both methods produce dense coatings (low porosity) with excellent adherence to the substrate and minimize oxidation during the application.

Other thermal-spray processes have been developed such as the high velocity oxygen fuel (HVOF) and the detonation gun methods to produce dense coatings with a good adherence to the substrate. These spray processes are also much more economical and convenient than VPS and EB-PVD methods. More recently, the new high frequency pulse detonation thermal-spray process (HFPD) represents a cost-effective alternative for the production of premium quality coatings.[4]

In this paper, the high temperature oxidation behavior in a simulated gas turbine environment at a temperature of 1000 °C of two MCrAlY coatings produced by the HFPD is analyzed.

1.1. HFPD Process

The HFPD spray system is based on a carefully designed gun able to produce a discontinuous behavior (cycled explosions) from a continuous supply of the detonatable gases and the powders. The system lacks mechanical moving parts, being designed with aerodynamic valves that allow the self-generation of discrete batches of gases and powders for each cycle, opening up the possibility of working in a wide range of explosion frequencies (up to more than 100 Hz) and gas mixtures. In the HFPD process, the flow of gaseous products from cycled explosions in the gun is used to accelerate and heat the sprayed particles. Typically, these particles attain very high speeds and sufficiently high temperatures leading to quite dense, well-bonded coatings from most commercially available powders (cermets, metallic alloys and ceramics).[5]

F.J. Belzunce, Materials Science Department, University of Oviedo, 33203 Gijón, Spain; and **V. Higuera, S. Poveda,** and **A. Carriles,** Energy Department, University of Oviedo, 33203 Gijón, Spain. Contact e-mail: belzunce@etsiig.uniovi.es.

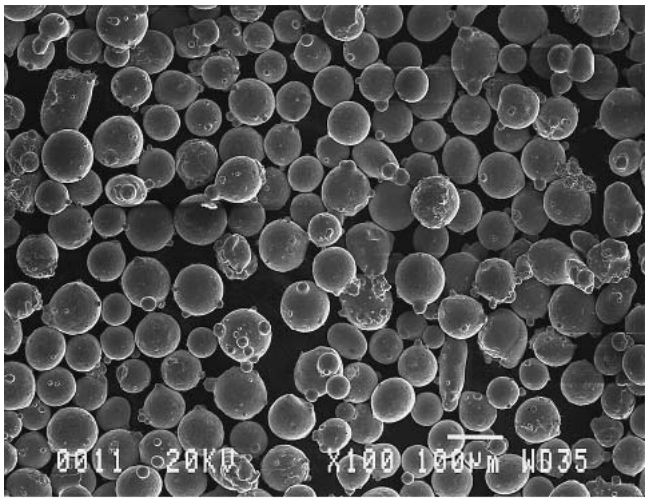

(a)

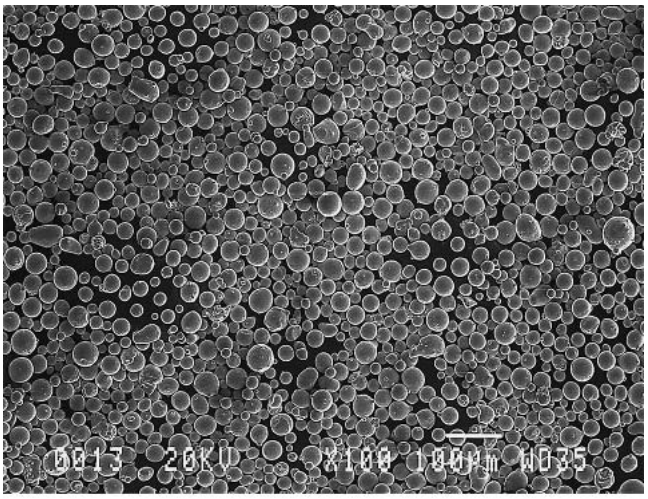

(b)

Fig. 1 Morphology of NiCrAlY and CoNiCrAlY powders

Table 1 Composition and Grain Size of the Powders

Powder	Ni, wt. %	Co, wt. %	Cr, wt. %	Al, wt. %	Y, wt. %	Size range, µm
NiCrAlY, gas atomized	balance	…	25	10	1	−106 + 56
CoNiCrAlY, gas atomized	32	balance	21	8	0.5	−62 + 11

One of the most important consequences of the particular physical process involved in the HFPD cycled explosions is the low consumption of gases, especially when compared with alternative continuous HVOF systems, mainly due to two factors: the different oxyfuel ratios (low oxygen) and the pulsed nature of the process. Another important economic consideration is its extended operating time and low maintenance needs.[4]

2. Experimental Procedure

Two types of commercial MCrAlY powders (Sulzer Metco, Switzerland) were sprayed onto an AISI 310 austenitic stainless steel by means of the HFPD thermal-spray method. The specimens were cylindrical with a diameter and height of 25 mm, in agreement with the ASTM C-633 Standard.[6] Table 1 shows the chemical composition and size range of both powders. The differences in morphology of both powders are better seen in Fig. 1.

A PK 200 HFPD thermal-spray apparatus (Aerostar Coatings, Irún, Spain) was used to spray both powders. The most relevant spraying parameters are listed in Table 2 along with the final coating thicknesses. Samples were first cleaned and blasted with alumina grit with an average size lower than 1 mm at 0.7 MPa, and their flat surfaces (25 mm diameter) were automatically thermal-spray coated immediately after cleaning.

The thickness of the coatings, along with their microstructure, porosity, and oxide content, were determined by optical microscopy techniques. The porosity and oxide content of the coatings were evaluated by point counting under an optical microscope in accordance with the ASTM E-562 Standard,[7] and the Vickers microhardness test was also performed on the coating layers using a load of 300 g. The phase composition of the coatings was determined by x-ray diffraction analysis using a Philips PW 1729-1710 (Amsterdam, The Netherlands) device equipped with a copper anode.

Table 2 Spraying Parameters

Spraying System: HFPD-PK200	NiCrAlY	CoNiCrAlY
Oxygen, 1/min	135	110
Nitrogen, 1/min	25	120
Fuel, 1/min	47 (propylene)	80 (natural gas)
Carrier gas, N_2, 1/min	20	20
Frequency, Hz	45	75
Spraying distance, mm	150	150
Powder feeding, g/min	26	30
Translation velocity, cm/s	10	10
Gun length: 250 mm Internal diameter: 20 mm		

High temperature cyclic oxidation tests were carried out in a 300 kW experimental combustor specially designed to attain temperatures as high as 1300 °C in environments that simulate the operating conditions of gas-fired gas turbine combined-cycle systems very closely (Fig. 2). The heating system of the combustor uses propane and air, previously heated with the flue gas stream generated in the combustion reaction. The atmosphere free oxygen content can be regulated, and a value of 11 vol.% was selected in our experimental tests to reproduce the most oxidizing conditions reported in these installations,[8] which was determined with a computerized gas analyzer. To simulate the operating conditions of the first stage blades of gas turbines, the tested samples were internally cooled with air (0.4-0.5 bar), thus obtaining a temperature difference of 100-200 °C between the surface of the samples and an internal region located at 1-2 mm. Figure 3 shows the sample geometry used in the experimentation and the location of two thermocouples used to measure the coating and substrate temperatures. Two similar samples were tested simultaneously.

The experiments were performed at an atmosphere temperature of 1000 °C during different time periods: 1, 2, 4, 8, 20, 40, and 160 h, with the ultimate aim of determining the progression of coating damage as well as the oxidation kinetics of these coatings. All the experiments of more than 8 h were carried out by repeating an 8 h cycle several times until the total time of exposure was attained. As shown in Fig. 4, average cycle heating and cooling rates of 30 and 12 °C/min were also measured in these tests and a temperature difference of about 150 °C was always maintained between coating and substrate. At the end of each test, the sample weight gain due to surface oxygen intake was determined using a balance with a sensitivity and accuracy of 0.1 mg.

All the specimens were nickel plated after the oxidation tests to preserve the surface oxide layer and were then diametrically cut, mounted in a plastic resin, ground, and polished. Finally, optical microscopy evaluation, x-ray diffraction (XRD), scanning electron microscopy (SEM) (JEOL 6100, JEOL LTD, Tokyo, Japan) and x-ray energy dispersive analysis (EDS) (Link EXL-1000, Oxford, UK) were performed to assess the structural changes and coating damage produced during high temperature oxidation testing.

3. Results and Discussion

Figure 5(a) and (b) shows the microstructure of NiCrAlY and CoNiCrAlY coatings in the as-sprayed condition. Both images show a low level of porosity. NiCrAlY powders exhibited a much larger grain size than CoNiCrAlY powders did; hence most of the projected particles were unable to melt completely during the spraying flight, giving rise to a lower density coating layer with many unmelted particles, some irregular porosity, and a lack of homogeneity. On the other hand, the CoNiCrAlY powders had a more appropriate grain size for spraying by means of this low temperature procedure, and a denser coating was obtained, although greater internal oxidation was measured in the as-sprayed condition due to the smaller particle size (Fig. 5).

Table 3 shows the total coating thickness, porosity, oxide content, and Vickers microhardness measured for both coatings in the as-sprayed condition and after different oxidation periods at 1000 °C. Porosity and hardness do not vary significantly with oxidation time. After 160 h exposure the hardness of NiCrAlY and CoNiCrAlY coatings, respectively, decreases and increases lightly, though finally, after long oxidation exposure times, the hardness of both coatings is equivalent. On the other hand, CoNiCrAlY coatings maintain their thickness, but NiCrAlY coatings show a slight decrease in thickness during the oxidation experiments due to the higher porosity and lack of homogeneity, which have been shown in these coatings. The internal oxidation of these coatings increases significantly after a very short oxidation time (first hour), but then, according to the data shown in Table 3, does not change any more. The oxidizing atmosphere penetrates the coatings through their open porosity, and when all the accessible internal surfaces have been oxidized, the process apparently stops. Subsequently, the oxidation phenomenon takes place only on the external surface of the coating in contact with the atmosphere, so that the presence of a surface protective layer is needed to avoid further oxidation. Figure 6 shows the external oxide layer as well as the internal oxidation of NiCrAlY and CoNiCrAlY coatings after 80 h at 1000 °C; while the NiCrAlY coating has its internal oxidation concentrated around its porosity, the CoNiCrAlY coating

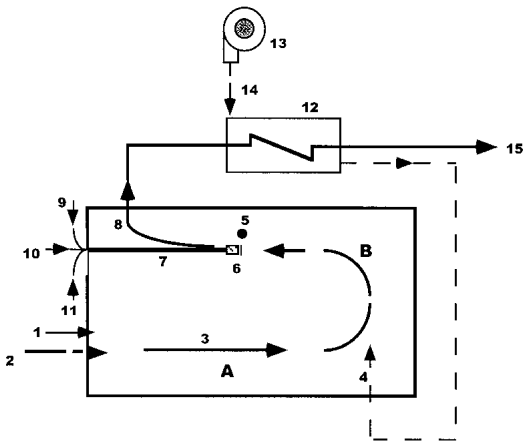

1._fuel gas (propane)
2._primary combustion air at room temperature
3._flue gas (first pass)
4._preheated air (secondary air)
5._flue gas sample
6._specimens
7._carrier specimens , thermocouples and cooling tubes
8._exhaust gas
9._thermocouple (substrate temperature)
10._ thermocouple (coating temperature)
11._cooling air inlet from compressor
12._air heater
13._secondary air fan
14._secondary air
15._exhaust gas to atmosphere
A._first flue gases pass (combustion zone)
B._second flue gases pass (dilution zone)

Fig. 2 Experimental combustor used in the oxidation tests

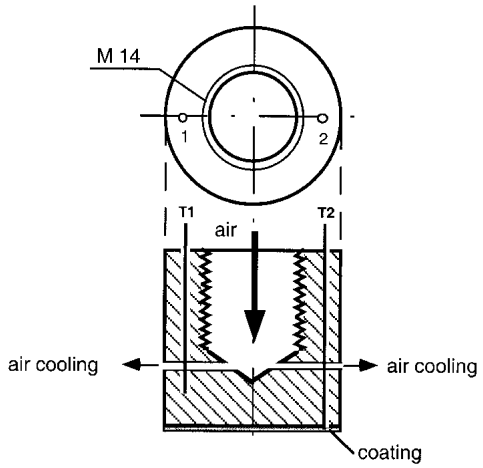

1._ Substrate temperature (T 1)
2._ Coating temperature (T 2)

Fig. 3 Specimen geometry showing air cooling system and thermocouple location

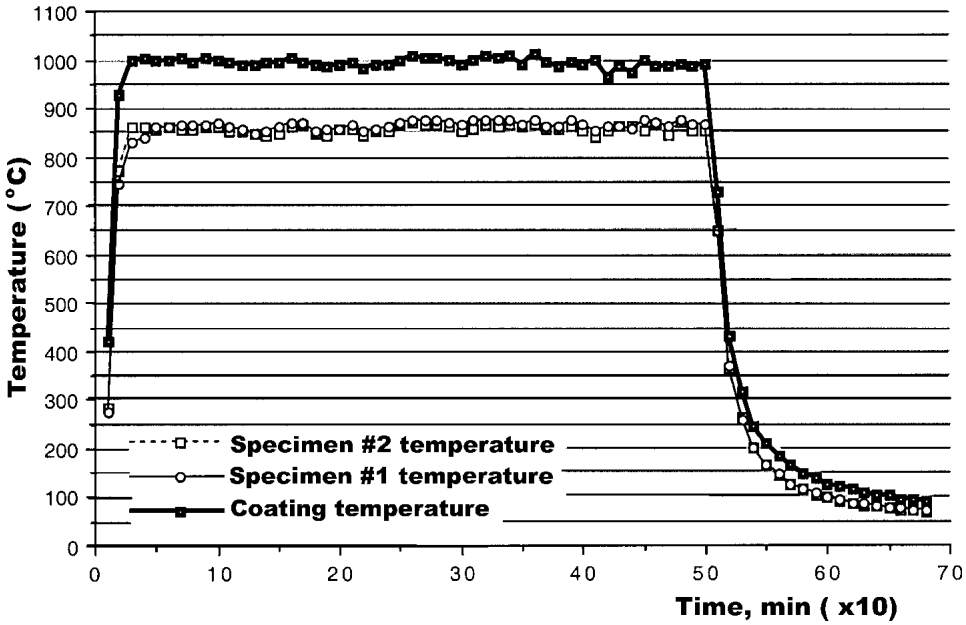

Fig. 4 8 h thermal cycle showing coating and substrate temperatures

Table 3 Coating Parameters Modification After Different Oxidation Times at 1000 °C (± Standard Deviation)

	As-Sprayed	1 h	2 h	4 h	8 h	40 h	80 h	160 h
NiCrAlY								
Thickness, μm	180 ± 20	145 ± 15	130 ± 25	130 ± 15	130 ± 20	120 ± 15	150 ± 25	130 ± 40
Porosity, %	2.6 ± 0.8	1.4 ± 0.4	1.7 ± 0.5	2.4 ± 0.7	2.3 ± 0.8	2.5 ± 0.5	2.1 ± 0.7	2.8 ± 0.5
Internal oxidation, %	0.4 ± 0.2	8.3 ± 2.5	6.4 ± 0.8	7.3 ± 1.6	7.8 ± 1.2	7.1 ± 1.7	7.9 ± 1	9 ± 1.5
HV_{300}	433 ± 40	490 ± 60	500 ± 50	470 ± 40	480 ± 35	435 ± 40	425 ± 25	385 ± 30
CoNiCrAlY								
Thickness, μm	180 ± 25	160 ± 15	155 ± 15	140 ± 20	165 ± 20	145 ± 20	160 ± 15	170 ± 15
Porosity, %	0.8 ± 0.2	0.9 ± 0.5	1.3 ± 0.5	0.4 ± 0.3	0.4 ± 0.4	1.4 ± 0.3	1.4 ± 0.4	1.1 ± 0.3
Internal oxidation, %	1.4 ± 0.3	10.4 ± 2.6	9.3 ± 1.5	8.5 ± 0.8	10.4 ± 1.7	7.3 ± 1.1	6.2 ± 1.6	6.1 ± 2.0
HV_{300}	320 ± 20	415 ± 50	415 ± 40	410 ± 40	395 ± 40	395 ± 30	385 ± 35	365 ± 30

has a more finely dispersed oxide network. Figure 7 shows the continuous oxide layer built up on the surface of one of these coatings (NiCrAlY after 160 h of oxidation). Two continuous layers of oxides were seen in some areas under the SEM. According to the analysis carried out using the electronic microprobe, the inner layer, which has a uniform thickness, is alumina, and the exterior layer, which was intermittently present and also has a more irregular morphology, is the corresponding mixed spinel-type oxide ($NiAl_2O_4$ and $CoAl_2O_4$, respectively). Similar results were obtained by other authors when characterizing the oxidation behavior of low-pressure plasma-sprayed MCrAlY coatings.[9-11] The presence of alumina and mixed spinel-type oxides was also revealed from the diffraction pattern of the surface of these samples as can be seen in Fig. 8, which corresponds to the NiCrAlY sample after 80 h in the combustor. It is the dense and continuous alumina layer that prevents inward diffusion of oxygen and explains the excellent resistance of these coatings against oxidation. It must also be remarked that no surface cracks or internal cracks were detected after any of the high temperature oxidation tests.

Figure 9 represents the weight change per unit surface of the NiCrAlY and CoNiCrAlY coatings measured during the 1000 °C oxidation tests. As only the flat surface of the samples were spray-coated (Φ 25 mm), it was not possible to obtain the net weight gain of the coatings. These data can be used only qualitatively, since at this temperature (1000 °C), the chromium oxide (Cr_2O_3) developed on the sample steel surface transforms into the volatile oxide CrO_3.[12] This fact may explain the weight loss observed in all the samples after long exposures at 1000 °C. Thus, the only point that can be deduced from Fig. 9 in relation to the oxidation behavior of both coatings is that, assuming the weight loss due to the formation of CrO_3 is the same for both coatings (no spalling has been detected), the apparently higher oxidation resistance characteristic of the CoNiCrAlY coating as its total weight loss was always greater (lower sample net weight).

Since the kinetics of the oxidation reaction cannot be obtained by weight measurements, the thickness of the Al_2O_3 layer was accurately measured under the SEM after different oxidation periods. The oxidation kinetics of the coatings obeys a parabolic rate law and are both quite similar (Fig. 10), giving rise to the parabolic rate constants shown in Table 4. K_1 expresses the

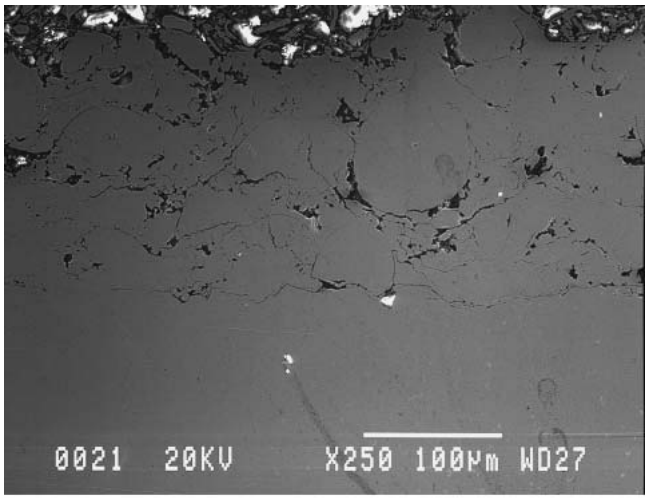

(a)

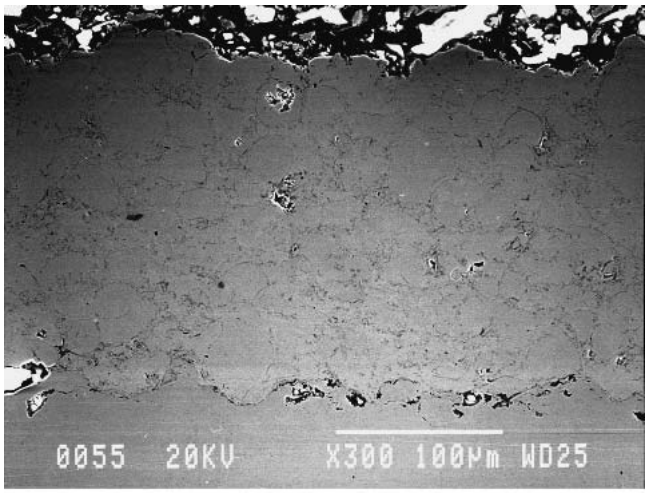

(b)

Fig. 5 As-sprayed coatings: **(a)** NiCrAlY and **(b)** CoNiCrAlY

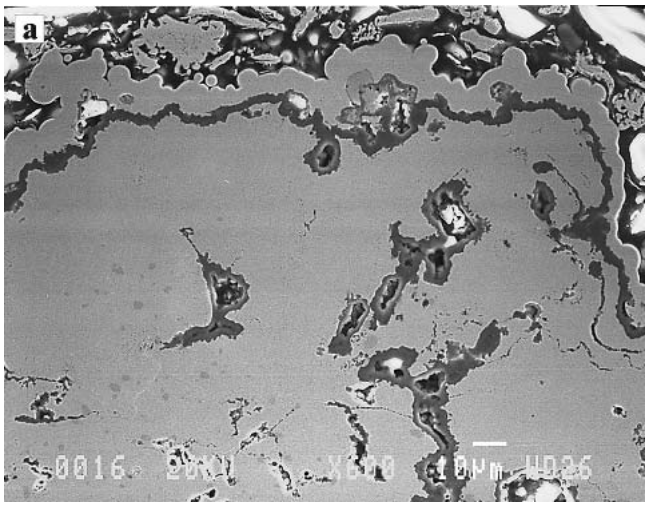

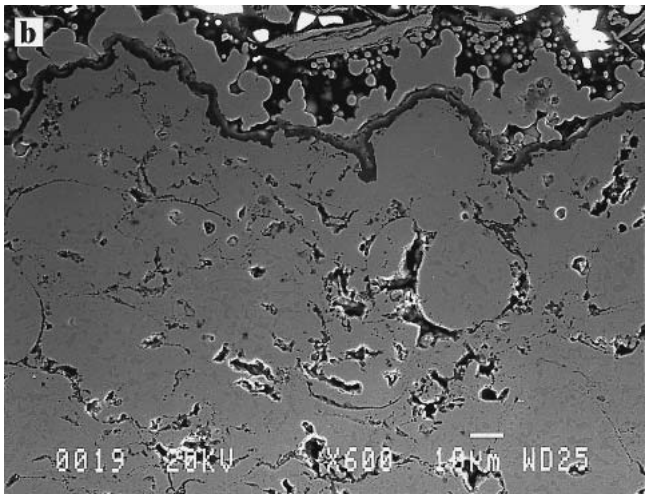

Fig. 6 Oxidation of coatings after 80 h at 1000 °C: **(a)** NiCrAlY and **(b)** CoNiCrAlY

oxidation behavior in terms of the alumina thickness, and K_2, the same behavior in terms of oxygen gain per unit coating surface (the density of pure alumina used in the calculation of K_2 was, in accordance with Ref. 13, 3.86 Mg/m^3). These parabolic rate constants are usually used as a measure for the growth rate of oxide; the behavior of the CoNiCrAlY coating thus seems to be slightly better. The parabolic rate constants obtained in this study present values very close to those measured for the formation of aluminum oxide on bulk nickel or cobalt based alloys under oxygen or air atmospheres.[14, 15]

4. Conclusions

NiCrAlY and CoNiCrAlY coatings may be thermal-sprayed using the HFPD process. The coatings are dense and exhibit small, interconnected porosity along particle boundaries. During high temperature cyclic oxidation in a simulated gas turbine atmosphere, the oxidizing atmosphere penetrates into the coatings

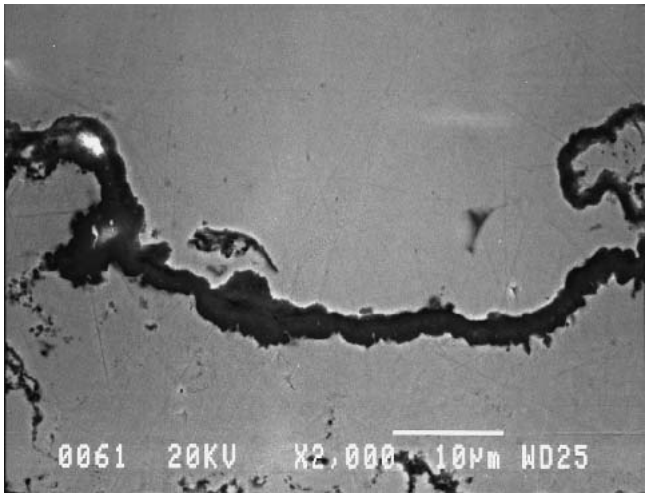

Fig. 7 Al_2O_3 layer built up on the surface of the NiCrAlY coating after 160 h oxidation

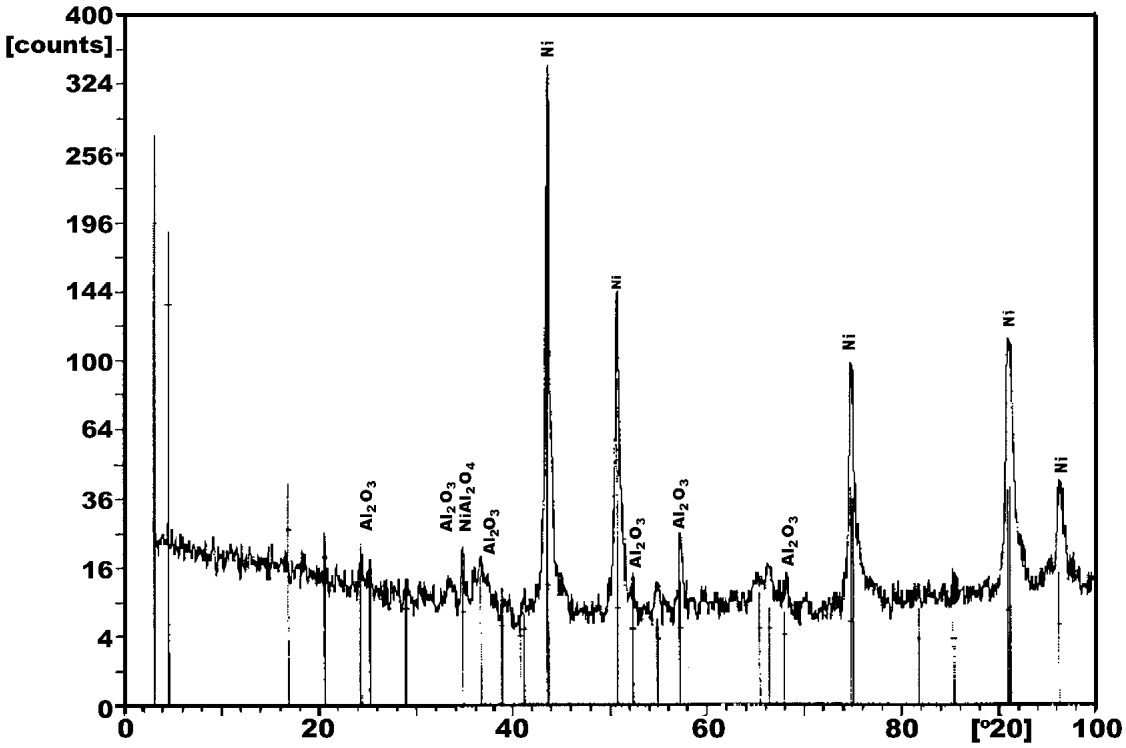

Fig. 8 Diffraction pattern of the surface of NiCrAlY coating (after 80 h of oxidation)

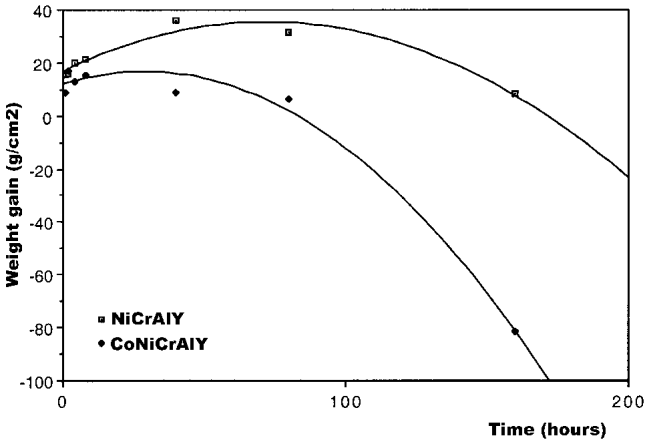

Fig. 9 Weight gain per unit surface (g/cm^2) of NiCrAlYand CoNiCrAlY coatings

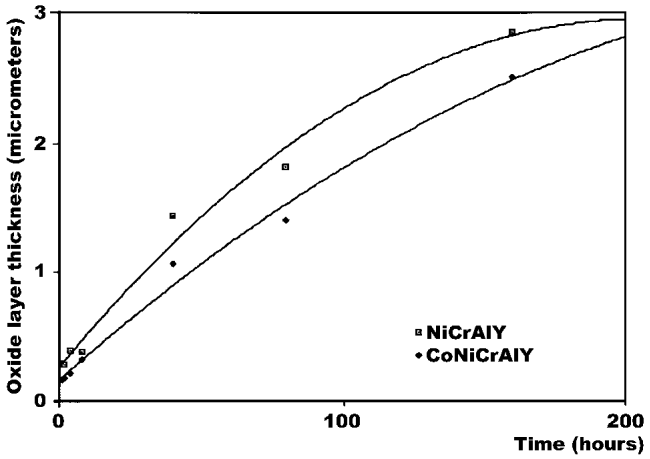

Fig. 10 Coating oxidation kinetics in air at 1000 °C (thickness of alumina layer, in μm, vs time)

through their open porosity; this internal oxidation occurs until all the accessible internal surfaces are oxidized. Subsequently, oxidation takes place only on the external surface, where a continuous and uniform layer of alumina protects the coating from further oxidation.

The CoNiCrAlY coating exhibited a slightly better behavior than NiCrAlY, manifested by a lower growth rate of the protective alumina layer. The more appropriate size range of CoNiCrAlY powders produces a more homogeneous microstructure, and this is the main reason that justifies this behavior.

Finally, the kinetics of the oxidation reaction could be determined only indirectly by measurements of the thickness of the Al_2O_3 layer. The oxidation kinetics of the coatings is parabolic and can be characterized by parabolic rate constants that are very similar to those measured for the formation of aluminum oxide on bulk nickel or cobalt based alloys reported in air and oxygen.

Table 4 Oxidation Parabolic Constants of HFPD Thermal-Sprayed Coatings

Parabolic Constants	NiCrAlY	CoNiCrAlY
K_1, μm^2/h	0.050	0.038
K_2, mg^2/cm^{4}s	2.07×10^{-6}	1.57×10^{-6}

Acknowledgments

Funding for this work was provided by FICYT (Asturias, Spain), Project Reference Number PB-MAT 98-03. The authors would also like to thank Aerostar Coatings for the provision of the coated samples.

References

1. W.P.Parks, E.E.Hoffman, W.Y.Lee, and I.G. Wright: "Thermal Barrier Coatings in Advanced Land-Based Gas Turbines," *J. Therm. Spray Technol.,* 1997, *6*(2), pp.187-92.
2. T. Haubold, J. Wigren, and C. Gualco: "Comparison of Thermal Cycling Experiments on Thick Thermal Barrier Coatings" in *Thermal Spray: Meeting the Challenges of the 21st Century*, C. Coddet, ed., ASM International, Materials Park, OH, 1998, pp. 22-27.
3. N. Czech, W. Esser, and F. Schmitz: "Developments in Materials for Gas Turbine Blades," *Siemens Power J.,* 1994, *4,* pp. 22-27.
4. I. Fagoaga, G. Barykin, J. De Juan, T. Soroa, and C. Vaquero, "The High Frequency Pulse Detonation (HFPD) Spray Process" in *Proc. United Thermal Spray Conf.,* C. Coddet, ed., ASM International, Düsseldorf, Germany, 1999, pp. 282-87.
5. I. Fagoaga, G. Barykin, J. De Juan, T. Soroa, C. Vaquero: "High Frequency Pulse Detonation (HFPD): Processing Parameters" in *Proc. United Thermal Spray Conf.,* C. Coddet, ed., ASM International, Düsseldorf, Germany, 1999, pp. 726-30.
6. Anon: "ASTM C-633, Standard Method for Adhesion or Cohesive Strength of Flame-Sprayed Coatings" in *Annual Book of ASTM Standards,* American Society for Testing and Materials, Philadelphia, PA, 1969, pp. 636-42.
7. Anon: "ASTM E-562, Standard Test Method for Determining Volume Fraction by Systematic Manual Point Count" in *Annual Book of ASTM Standards,* Vol. 03.01, American Society for Testing and Materials, Philadelphia, PA, 1990, pp. 583-88.
8. R. Chellini: "The Integrated Gasification, Combined-Cycle Plant at Puertollano," *Diesel & Gas Turbine Worldwide,* Oct 1997, pp. 12-14.
9. J. A. Haynes, E.D. Rigney, E.D. Ferber, and W.D. Porter: "Oxidation and Degradation of a Plasma-Sprayed Thermal Barrier Coating System," *Surf. Coat. Technol.,* 1996, *86-87,* pp. 102-08.
10. N. Czech, V. Kolarik, W.J. Quadakker, and W. Stamm: "Oxide Layer Phase Structure of MCrAlY Coatings," *Surf. Eng.,* 1997, *13*(5), pp. 384-88.
11. E.A.G. Shillington and D.R. Clarke: "Spalling Failure of a Thermal Barrier Coating Associated With Aluminum Depletion in the Bond-Coat," *Acta Mater.,* 1999, *47*(4), pp. 1297-1305.
12. N. Birks and G.H. Meier, *Introduction to High Temperature Oxidation of Metals,* Edward Arnold Pub., London, United Kingdom, 1983, pp. 80-83.
13. Anon: *ASM Engineered Materials Reference Book,* ASM International, Metals Park, OH, 1989, pp 168-69.
14. H. Iwamoto, T. Sumikawa, K. Nishida, T. Asano, M. Nishida, and T. Araki: "High Temperature Oxidation Behavior of Laser Clad NiCrAlY Layer," *Mater. Sci. Eng.,* 1998, *A241,* pp. 251-58.
15. R. Peraldi, D. Monceau, A. Malie, and B. Pieraggi: "High Temperature Oxidation of Bond Coats in Thermal Barrier Systems" in *Thermal Spray: Meeting the Challenges of the 21st Century*, C. Coddet, ed., ASM International, Materials Park, OH, 1998, pp. 1561-64.